Jurnal Ilmu Fisika
Vol. 17, No. 2, September 2025, pp. 110–124
ISSN: 1979-4657 (Print); 2614-7386 (Online)
https://doi.org/10.25077/jif.17.2.110-124.2025

Developing Surface Rainfall Data Based on Blending of Satellite-Based Products and Rain Gauge Observations in the Ngawi Region, East Java

Joko Budi Utomo[1,2], Eko Yuli Handoko[1*], Muhammad Aldila Syariz[1], Ardhasena Sopaheluwakan[2]
[1] Department of Geomatics Engineering, Institut Teknologi Sepuluh Nopember, 60111, Surabaya, Indonesia
[2]Agency for Meteorology Climatology and Geophysics (BMKG), 10610, Jakarta, Indonesia

Article Info

Article History:

Received March 04, 2025
Revised May 02, 2025
Accepted May 03, 2025
Published online May 05, 2025

Keywords:

Surface Rainfall
Satellite product
Kriging
Rain gauge
Leave-one-out cross validation

Corresponding Author:

Eko Yuli Handoko,
Email: ekoyh@its.ac.id

ABSTRACT

Rainfall estimation can be performed using various methods, including direct satellite observations (RR-Satellite). However, these estimates show discrepancies when compared to actual observations in-situ rain gauges (RR-Obs). To address this challenge, one potential solution is integrating RR-Satellite with RR-Obs. The Kriging with External Drift (*KED*) interpolation method is a blending technique that incorporates RR-Satellite as external drift. This study utilized four satellite dataset, namely CHIRP, CMORPH, GSMAP_V8, and IMERG as auxiliary information to generate monthly rainfall estimates (RR-Blended) at 26 rain gauges in Ngawi, East Java, for the period 2001 - 2023. The performance of each satellite dataset was evaluated using Leave-One-Out Cross Validation (LOOCV). The results indicated that RR-Blended using CHIRP (bCHIRP) demonstrated the best accuracy at the climatological scale, with KGE > 0.3 and TSS > 0.65, outperforming other satellite dataset. At the monthly scale, bCHIRP, bCMORPH, and bIMERG showed better performance in different months throughout the year. In terms of spatial accuracy, bCMORPH achieved the highest performance. Our findings suggest that each satellite offers unique advantages based on the time and location of observation. Therefore, we recommend using a weighted combination of RR-Blended from four satellites as the most effective approach for obtaining the best rainfall estimates.

1. INTRODUCTION

The accuracy of climate variability analysis relies on precise rainfall measurements obtained from in-situ observations using rain gauges. Despite being regarded as the most precise means of estimating rainfall (Beck et al., 2019), these instruments are still subject to biases or errors that may compromise measurement accuracy, influenced by wind, evaporation, wetting, splashes, and factors associated with the instruments and human observations (Kurniawan, 2020; Michelson, 2004). Furthermore, achieving sufficient coverage for accurate rainfall monitoring using rain gauges remains a challenge, particularly due to regional variability (Vernimmen et al., 2012)

To address the geographical coverage constraints of in-situ rain gauges, satellite-based rainfall has been available in recent decades for monitoring rainfall in all global regions (Hou et al., 2014; Fatkhuroyan & TrinahWati, 2018; Pratama et al., 2022). Rainfall satellites employ microwave sensors to detect radiation emissions and scattering from raindrops, subsequently correlating these measurements to rainfall intensity using a model (Kubota et al., 2007; Hou et al., 2014; Goshime et al.,

2019). Satellite products have demonstrated favorable outcomes, and in some settings, they may be comparable to or exceed reanalysis data (Beck et al., 2017).

Several studies have explored satellite-based rainfall data in Indonesia, highlighting their effectiveness in monitoring precipitation patterns across the region. For example, the study by Ramadhan et al. (2022) assessed the performance of the Global Precipitation Measurement Integrated Multi-Satellite Retrievals (GPM IMERG) in Indonesia, demonstrating its ability to provide reliable precipitation-amount-based and precipitation-frequency-based indices. In another study, Ramadhan et al. (2023) evaluated the near-real-time data from the Global Satellite Mapping of Precipitation (GSMAP), showing its potential for observing rainfall with faster latency, which is particularly beneficial for real-time monitoring in Indonesia. Additionally, Wati et al. (2021)found that the Climate Prediction Center Morphing Technique (CMORPH) consistently underestimated rainfall across various temporal scales in Indonesia, showing a negative bias in its estimates. Similarly, Bai et al. (2018) and Pratama et al. (2022) highlighted that the Climate Hazards Group Infrared Precipitation Satellite with Station (CHIRPS) often produced inflated precipitation estimates, especially in areas of heavy rainfall.

Rain gauge and satellite-based rainfall data each have their own limitations, which can affect the accuracy and completeness of rainfall monitoring rain gauges offer high accuracy at specific locations but are often limited by missing data due to equipment failure, environmental factors, or irregular maintenance (Groisman & Legates, 1994; Peterson et al., 1998; Michelson, 2004; Michaelides et al., 2009). In contrast, satellite data provides broad spatial coverage but may have lower resolution and be affected by atmospheric conditions such as cloud cover (Jiang et al., 2019). To overcome these limitations, combining or blending both data sources can produce a more accurate and comprehensive rainfall dataset, improving the reliability of rainfall analysis and monitoring (Chappell et al., 2013; Shen et al., 2019; Muharsyah et al., 2021; Chua et al., 2022)**.**

Blending satellite and in-situ observations improves rainfall estimates by combining the strengths of both data sources (Verdin et al., 2015; Shen et al., 2019; Muharsyah et al., 2021; Chua et al., 2022). This method is especially useful in areas with few rain gauges (Lin & Wang, 2011). Studies by Jewell & Gaussiat (2015) and Nanding et al. (2015) showed that Kriging with External Drift (*KED*) better preserves the spatial distribution of rainfall than Ordinary Kriging. Lin & Wang (2011) also found that combining satellite data with ground observations through conditional kriging reduces bias and improves accuracy in regions with limited rain gauges. Chappell et al. (2013) and Chua et al. (2022) used Empirical Bayesian Kriging Regression Prediction to blend GSMAP data with rain gauges in Australia, yielding better estimates than Ordinary or Simple Kriging, particularly in areas with complex topography and sparse gauges. Based on these findings, *KED* was chosen for this study for its ability to integrate satellite data, improve spatial accuracy, and reduce errors in regions with limited observational data.

This study aims to evaluate the performance of various satellite products in improving rainfall estimation through *KED*, with the goal of identifying the most suitable satellite data for use as auxiliary input. By doing so, this research seeks to produce more accurate and reliable gridded rainfall dataset that better capture the spatial and temporal variability of rainfall. Additionally, the study aims to highlight the strengths and limitations of existing satellite products to support the selection process for operational use. Ultimately, the goal is to develop an improved blended gridded rainfall dataset that surpasses the performance of standalone satellite products, thereby enhancing rainfall monitoring capabilities in Indonesia. To the best of our knowledge, this is the first study to assess the use of multiple satellite sources for rainfall estimation through a *KED*-based blending approach in the Indonesian context. The findings are expected to support BMKG for generating high-quality gridded rainfall products**.**

2. DATA AND METHODS

2.1 Observational Data and Study Area

This study examines the Ngawi Region in East Java Province, which borders Madiun, Ponorogo, Magetan, and Bojonegoro Region. Ngawi is located between 7°26'15" - 8°02'20" S and 111° 29'15" -

112° 15'15" E. This region exhibits diverse geography, featuring mountains in the southwest and south, alongside lowlands in the north and east. Ngawi experiences annual rainfall of approximately 1936 mm/year, which typically has a rainy season from November to April (Mulsandi et al., 2024). This study uses monthly rainfall (RR) in mm/month from 2001 to 2023 (23 years) at 26 rain gauges (Figure 1). The data source was obtained from BMKGSoft, a database management application used internally by BMKG for storing and organizing meteorological observation data. Before processing, the data underwent Quality Control (QC) with the identical methodology employed to generate the 1991-2020 rainfall normal map (BMKG, 2021). All the rain gauges used in this study have more than 95% data completeness, ensuring the validity and accuracy of the information used.

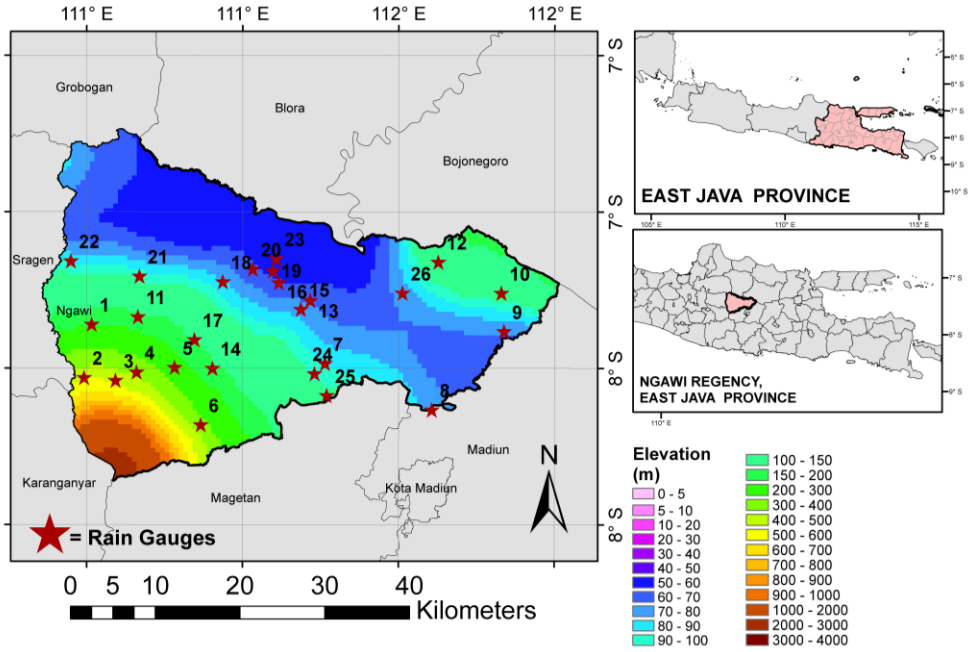

Figure 1. The study area in Ngawi, East Java, Indonesia, is depicted, featuring 26 rainfall stations (denoted by red stars) overlaid with elevation data in meters.

2.2 Satellite Data

This study involved four satellites, and the data were acquired in the NetCDF format and included varying resolutions. The satellite data is accessible for free and can be downloaded from the locations shown in Table 1. GSMAP is a project initiated by the Japan Science and Technology Agency (JST) in 2002 and further developed by the Japan Aerospace Exploration Agency (JAXA) through the Precipitation Measuring Mission (PMM) program since 2007 (Kubota et al., 2007). CHIRP uses Thermal Infrared Cold Cloud Duration (TIRCCD) data to estimate precipitation. A fixed threshold of 235°K is used to distinguish the occurrence of the precipitation. GPM IMERG is a satellite that has global rainfall data developed by NASA and JAXA (Huffman et al., 2019). GPM IMERG has a spatial resolution of 0.1° × 0.1°, while its temporal resolution is hourly. CMORPH or CPC Morphing Technique is a satellite-based system developed by NOAA's Climate Prediction Center (CPC) to estimate rainfall (Joyce et al., 2004). CMORPH uses infrared satellite data from the GOES and METEOSAT satellites, as well as radar data. The spatial resolution of CMORPH is 0.25° × 0.25°, while its temporal resolution is every 3 h.

2.3 Methodology

The blending technique proposed in this study refers to rainfall estimation using the Kriging with External Drift (*KED*) interpolation method. Four satellite products, namely CHIRP, CMORPH, GSMaP_V8, and IMERG, were selected as drift or auxiliary variables to support the estimation of

monthly rainfall (RR) in Ngawi. In general, the research process begins with estimating monthly rainfall using the *KED* approach by applying the Leave-One-Out Cross-Validation (LOOCV) method (Cantet, 2017; Pang et al., 2023). Through this method, blended rainfall estimates which referred to as RR-Blended were produced at 26 rain gauge locations. These estimates represent the output of the *KED* interpolation process that blends in-situ rain gauge data with satellite rainfall data. Each satellite produced a distinct RR-Blended dataset, abbreviated as bCHIRP, bCMORPH, bGSMAP_V8, and bIMERG. For comparison, the monthly RR values were also directly extracted from each satellite at the same 26 locations using the nearest-neighbor method. These direct satellite-derived values are referred to as RR-Satellite. Both the RR-Blended and RR-Satellite dataset were treated as simulated rainfall values for further validation and analysis

Table 1 List of satellites used in this study

Satellite	Data Source Link	Resolution Spatial (Temporal)	Reference
CHIRP, The Climate Hazards Group Infrared Precipitation Satellite	https://data.chc.ucsb.edu/products/CHIRP/daily/netcdf/	0.05º x 0.05º (daily)	Funk et al. (2015)
CMORPH, Climate Prediction Center morphing technique	https://www.ncei.noaa.gov/data/cmorph-high-resolution-global-precipitation-estimates/access/daily/0.25deg/	0.25º x 0.25º (daily)	Joyce et al. (2004)
GSMAP_V8, Global Satellite Mapping of Precipitation, version 8	ftp://hokusai.eorc.jaxa.jp/realtime_ver/v8/daily0.1/00Z-23Z/	0.1º x 0.1º (daily)	Kubota et al. (2007)
IMERG, Global Precipitation Measurement Integrated Multi-Satellite Retrievals Final Version	https://apdrc.soest.hawaii.edu/dods/public_data/satellite_product/GPM_IMERG	0.1º x 0.1 º (daily)	Huffman et al. (2019)

2.3.1 Kriging With External Drift (*KED*)

KED is a variant of spatial interpolation that uses additional information in the estimation of the target variable at unobserved locations (Hengl et al., 2003; Sideris et al., 2014; Oliver & Webster, 2015). In the *KED*, rainfall estimation($Z_{KED}(x_0)$)at an unknown point is calculated as a weighted combination of the observed rainfall values at surrounding points. This process uses an equation written as follows:

$$Z_{KED}(x_0) = \sum_{i=1}^{n} \lambda_i^{KED} Z_g(x_i) \quad (1)$$

Where $Z_{KED}(x_0)$ is estimated rainfall at the point x_0; λ_i^{KED} is *KED* weight at the rain gauges points x_i; and $Z_g(x_i)$ is Observation rainfall value at the rain gauges point x_i

The semi-variogram model is a fundamental component of *KED*. The semi-variogram represents the degree of spatial dependency between variable values at different locations, which is essential for constructing a Kriging model (Oliver & Webster, 2015). In the Kriging model, the semi-variogram is transformed into a model function that allows for the prediction of variable values at unobserved locations by considering their proximity to the observed data points. The configuration of the semi-variogram model is defined by three key parameters: Nugget, Sill, and Range (Ly et al., 2011; Oliver & Webster, 2015). This study did not focus on testing these three parameters, as they were appropriately selected using the best estimates available in the *KED* module of PyKrige (Murphy et al., 2024). Additionally, the PyKrige module provides several options for the semi-variogram model, including spherical, exponential, power, linear, and Gaussian models. However, this study utilized the exponential model, which is generally known to produce more accurate value estimates compared to the other models (Novia Nur Rohma, 2022; Pririzki et al., 2022).

2.3.2 Validation Method and Metrics Evaluation

The Leave-One-Out Cross Validation (LOOCV) was used to assess the impact of each satellite on estimating the rainfall generated by the *KED*, similar to the approach employed by (Cantet, (2017). LOOCV involves partitioning the dataset into several folds equivalent to the total number of samples in the dataset. In each cycle, the dataset serves as the test (test set), while the remainder is utilized as training (training set). This procedure is repeated for the entire number of samples, ensuring that each data sample can serve as test data once. This study employed the LOOCV for each rain gauge (276 months x 26 locations). For example, to estimate the January 2001 RR-Blended at RG 1 (RG1 denotes rain gauges no.1 and same conventions applies to RG2 to RG26), the January 2001 RR-Obs values from locations other than gauges1, namely the RR-Obs at RG2, RG3, ..., RG26, are utilized as the training set. The procedure is repeated using RG1, RG3, ..., RG26 as the training set to estimate the January 2001 RR-Blended at RG2, continuing sequentially until RG26. Upon concluding January 2021 RR-Blended for all positions, replicate for the subsequent months, February 2021 to December 2023. Finally, we obtained the RR-Blended dataset for each satellite i.e. bCHIRP, bCMORPH, bGSMAP_V8, and bIMERG.

Table 2 List of statistical metrics used for the evaluation

Metrics	Equation	Range (Perfect)
Correlation	$CC = \frac{\sum_{i=1}^{n}(x_i - \bar{x})\,(y_i - \bar{y})}{\sqrt{\sum_{i=1}^{n}(x_i - \bar{x})^2}\sqrt{\sum_{i=1}^{n}(y_i - \bar{y})^2}}$	-1 to 1 (1)
RSME	$RMSE = \sqrt{\frac{1}{N}\sum_{i=1}^{n}(x_i - y_i)}$	0 to ∞ (0)
Kling Gupta Efficiency (KGE)	$KGE = 1 - \sqrt{(CC-1)^2 + \left(\frac{\sigma_x}{\sigma_y} - 1\right)^2 + \left(\frac{\bar{x}}{\bar{y}} - 1\right)^2}$	-1 to 1 (1)
Taylor Diagram Skill Score (TSS)	$TSS = \frac{4(1+CC)^4}{\left(CV_x + \frac{1}{CV_x}\right)^2 (1+CC_0)^4}$	0 to 1 (1)

where,

x	:	Simulation values, RR-Satellite or RR-Blended
y	:	Observation value, RR-Obs
N, n	:	Number of data (number of rain gauges for spatial scale or number of months/years for temporal scale)
CC	:	Correlation
CC_0	:	Maximum correlation between the simulated values
σ	:	Standard Deviation
CV	:	Coefficient variation or normalized Standard Deviation

Furthermore, the RR-Blended and the RR-Satellite were verified with RR-Obs to measure their capabilities. Four statistical metrics were employed: Correlation, RMSE, Kling-Gupta Efficiency (KGE), and Taylor Diagram Skill Score (TSS), as presented in Table 2. Correlation and RMSE, assessing the alignment of the pattern and the extent of the squared error. This study incorporates two additional metrics, KGE and TSS, to enhance the analysis. KGE is utilized to evaluate the efficacy of a predictive model. KGE is engineered for enhanced flexibility and is capable of addressing multiple facets of uncertainty and error inside the prediction model, encompassing systematic mistakes, temporal fluctuations, and correlations between forecasts and observational data (Knoben et al., 2019; Mathevet et al., 2023). The Taylor Skill Score (TSS) is a metric developed to quantify the accuracy of simulation results by integrating key statistical measures into a single value (Yang et al., 2020). It was derived from

the Taylor diagram, which was originally designed to visually represent the relationship among correlation, standard deviation, and bias between simulated and observed data (Taylor, 2001). The advantage of TSS lies in its disregard for the components of each model, as it incorporates the simulation results derived from other models. The TSS score indicates the comparative accuracy of one model relative to another.

3. RESULTS

3.1 RR-Satellite Error Rate

Ngawi is in southern Indonesia and is characterized by a rainy season (WET) and a dry season (DRY). Ngawi experiences a monsoonal rainfall pattern (Aldrian & Dwi Susanto, 2003), with the rainy season typically beginning in November and the dry season starting around May. This results in approximately six months of wet conditions and six months of dry conditions each year. Overall, the mean of the RR-Satellites of the 26 rain gauges in Ngawi has a climatological pattern similar to that of the RR-Obs (Figure 2a). The estimations from the four satellites effectively represent the rainfall patterns in Ngawi, particularly with the WET and DRY periods. All satellites, except for GSMAP_V8, concur that the WET and DRY periods transpire from November to April and from May to October, respectively. Nevertheless, the four satellites exhibited a bias that differed among each satellite (Figure 2b). GSMAP_V8 is frequently underestimated throughout the year, particularly during the early rainy season (January to April). Conversely, the remaining three RR-Satellites tended to overshoot consistently throughout the year. Besides GSMAP_V8, the remaining three RR-Satellites have positive biases that are generally more pronounced during the rainy season (November – March). The four satellites have a commonality in that they often possess an absolute bias above 50 mm/month during the WET and less than 25 mm/month during the DRY period. This indicates vulnerability, as the RR-Satellite estimation during the WET period exceeds that of the DRY period. This is typical because of the increased variability of rainfall in Indonesia throughout the WET period, particularly in regions characterized by monsoonal rainfall patterns (Aldrian & Dwi Susanto, 2003).

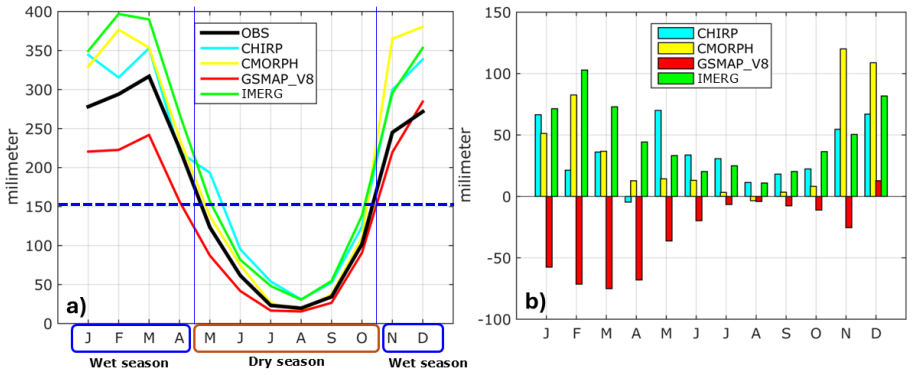

Figure 2 (a) Annual cycle (climatology) of rainfall for all rain gauges in Ngawi between RR-Obs and RR-Satellite; (b) Difference between RR-Obs and RR-Satellite each month. The horizontal blue line is the criteria for the rainy season and dry season (150 mm/month) based on BMKG's criteria.

3.2 Comparison of RR-Blended versus RR-Satellite

This section elucidates the impact of RR-Blended on *KED* outcomes overall. Upon completing the LOOCV method, we acquired a dataset equivalent in size to the observational data (26 locations x 276 months). Figure 3 demonstrates that RR-Blended can nearly flawlessly duplicate the observed pattern. RR-Blended can effectively calibrate the inflated value recorded by the RR-Satellite during the rainy season. The *KED* results enhance the accuracy of the satellite value estimation in both WET and DRY. Figure 3 illustrates the differences in RMSE values between the RR-Satellite and the RR-Obs, as

well as versus the RR-Blended and RR-Obs. Figure 3 shows the time-series of the monthly rainfall in the NGAWI_35210101 station. The RMSE value from 2001 to 2023 indicates that the monthly average for the RR-Satellite typically exceeds 100 mm/month. Simultaneously, the *KED* results indicate that the RMSE of RR-Blended is less than 100 mm/month, with a variance of up to 30 to 50 mm/month. Subsequently,

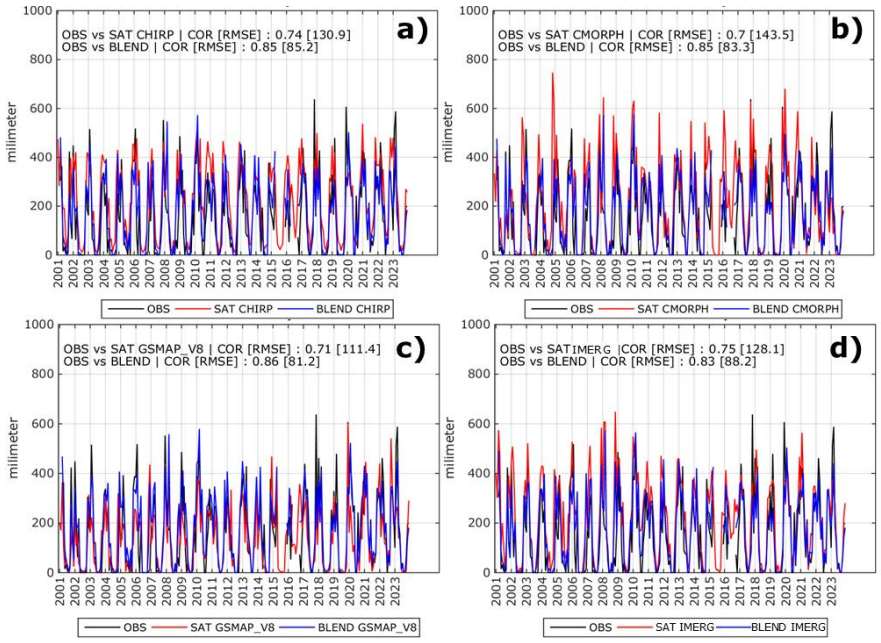

Figure 3 Time series pattern of RR-Obs (Black) compared to RR-Satellite (red) and RR-Blended (blue) at NGAWI rain gauges_35210101a_Blue Water_Tretes, for each satellite (a) CHIRP, (b) CMORPH), (c) GSMAP_V8 and (d) IMERG

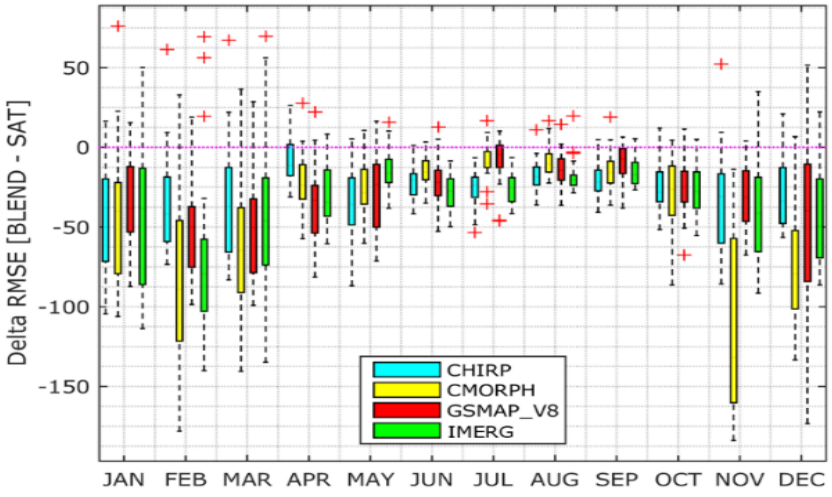

Figure 4 The decrease in RMSE value in each month between RR-Blended and RR-Satellite is shown, with the red cross mark representing the outlier delta value. A paired t-test has been conducted between RR-Blended and RR-Satellite, with the results indicating a significant difference, as the p-value is less than 0.05

Figure 4 illustrates the discrepancy in error levels between the RR-Blended and RR-Satellite dataset. The boxplot presented consolidates the delta error values across all rain gauges. Most delta

values are observed to fall below the zero line, indicating a substantial reduction in error for RR-Blended when compared to RR-Satellite (the pre-blended states). During the WET period, particularly in January and February, several rainfall gauges displayed delta errors as outliers, suggesting that in certain instances, the performance of RR-Blended did not exceed that of RR-Satellite. However, it is crucial to emphasize that these outlier values did not alter the overall conclusions of the analysis, as they represent an isolated portion of the data. These outliers were primarily observed at rain gauges located along the elevation slope, including gauges No. RG10, RG12, RG2, RG3, and RG6 (see Figure 1)

Moreover, the reduction in inaccuracy indicates that the correlation of RR-Blended higher than that of RR-Satellite (Figure 5). The four satellites exhibit nearly identical correlation enhancements across all stations. Generally, increments exceeding 0.15 are more prevalent in the GSMAP_V8 satellite. The explanation is that the capability of the RR-Satellite GSMAP_V8 (top panel of Figure 5c) is comparatively inferior to that of other satellites for most rain gauges in Ngawi. Figure 5 indicates that, in terms of correlation, the RR-Satellite has a relatively strong performance; nevertheless, the RR-Blended enhances the correlation further. The enhanced correlation shown in RR-Blended, as illustrated in Figure 3, is attributable to its superior capacity to capture high rainfall occurrences throughout the WET period. The results of Figures 3, 4, and 5 demonstrate that the performance of RR-Blended enhances the accuracy of the monthly rainfall estimations. This finding aligns with the studies of Jewell & Gaussiat, (2015) and Cantet, (2017), which indicate that *KED* enhances the precision of rainfall estimates.

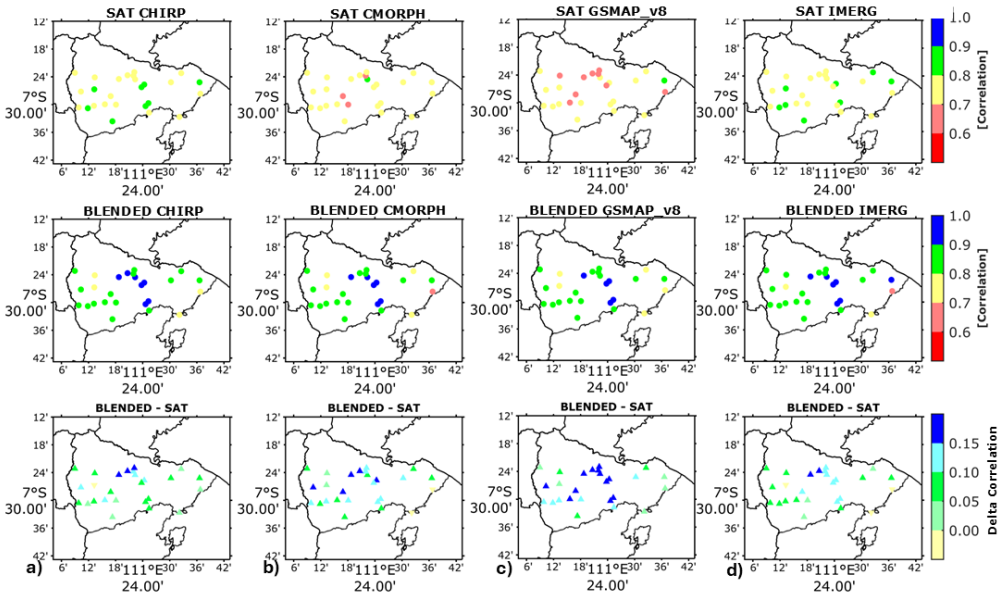

Figure 5 Correlation of each rain- between RR-Satellite versus RR-Obs values (top row panel), RR-Blended versus RR-Obs (middle row panel), and the difference in changes in correlation values for each satellite (a) CHIRP), (b) CMORPH, (c) GSMAP_V8, and (d) IMERG.

3.3 Climatology Assessment

Upon determining that the RR-Blended results yield superior estimates compared to the RR-Satellite, the subsequent step is to evaluate the efficacy of each satellite employed as auxiliary information on the *KED*. This section assesses the capability of satellites based on climatological data. Initially, consider the annual rainfall amount or the quantity of rain that accumulates over the course of a year. The average annual rainfall from 2001 to 2023 is represented by each rain gauge. The bCHIRP outperformed the others across all scores (Correlation, RMSE, KGE, and TSS), as illustrated in Figure 6 bIMERG ranks second, yielding commendable results, followed by b GSMAP_V8 and bCMORPH.

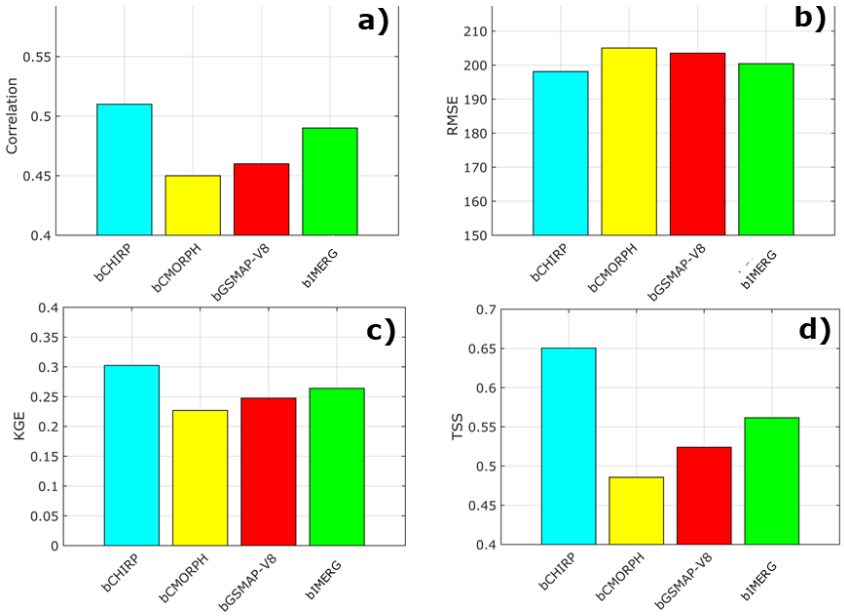

Figure 6 Skill scores (a) Correlation, (b) RMSE, (c) KGE) and (d) TSS of each RR-Blended for the four satellites

Table 3 Skill Scores per month of four RR-Blended. Values in dark gray cells indicate the best scores in each month. Bold text is the highest weight.

RR-Blended	Metrics	JAN	FEB	MAR	APR	MAY	JUN	JUL	AUG	SEP	OCT	NOV	DEC
bCHIRP	RMSE	34	38	39	34	22	13	8	7	8	22	30	24
	KGE	0.598	0.458	0.383	-0.095	0.053	-0.037	0.568	0.120	0.231	0.185	0.541	0.159
	TSS	0.851	0.684	0.827	0.536	0.704	0.348	0.738	0.354	0.428	0.345	0.781	0.369
bCMORPH	RMSE	38	37	39	35	22	12	8	7	8	20	29	23
	KGE	0.466	0.448	0.342	-0.277	0.056	-0.004	0.561	0.291	0.233	0.383	0.553	0.179
	TSS	0.617	0.680	0.747	0.232	0.708	0.385	0.777	0.690	0.425	0.729	0.825	0.394
bGSMAP_V8	RMSE	37	38	41	33	22	13	8	7	7	22	29	23
	KGE	0.499	0.443	0.280	-0.222	-0.004	-0.057	0.554	0.156	0.242	0.213	0.541	0.163
	TSS	0.659	0.649	0.595	0.283	0.555	0.309	0.723	0.418	0.442	0.395	0.799	0.358
bIMERG	RMSE	37	36	40	32	23	12	8	7	7	21	30	22
	KGE	0.428	0.499	0.319	-0.069	0.020	0.157	0.605	0.167	0.301	0.351	0.533	0.281
	TSS	0.579	0.774	0.675	0.607	0.630	0.723	0.806	0.427	0.565	0.655	0.786	0.598
WEIGHT	bCHIRP	**0.31**	0.245	**0.29**	0.32	**0.27**	0.2	0.24	0.19	0.23	0.16	0.24	0.21
	bCMORPH	0.23	0.244	0.26	0.14	0.27	0.22	0.26	**0.37**	0.23	**0.34**	**0.26**	0.23
	bGSMAP_V8	0.24	0.233	0.21	0.17	0.21	0.18	0.24	0.22	0.24	0.19	0.25	0.21
	bIMERG	0.21	**0.278**	0.24	**0.37**	0.24	**0.41**	**0.26**	0.23	**0.3**	0.31	0.25	**0.35**

3.4 Monthly Assessment

The previous climatology assessment did not clearly highlight the accuracy potential of the RR-Blended, especially with respect to its temporal resolution across different months. In Ngawi, rainfall variability follows a distinct pattern, with a WET period at the start of the year and a DRY period during

the mid-year. Therefore, it is important to assess the RR-Blended accuracy on a monthly basis. For each month, varying skill scores were obtained from the four satellites, as shown in Table 3. The correlation score has been excluded due to the generally similar values across the satellites.

Based on the three-evaluation metrics used, RMSE does not show significant variation among the satellites. The monthly differences in RMSE between the satellites are approximately 1–2 mm. However, for the other two metrics, KGE and TSS, considerable disparities are observed. The results indicate that CHIRP performs the best in January, March, and May, while bIMERG outperforms the others in February, April, June, July, September, and December. bCMORPH excels in August, October, and November. On the other hand, b GSMAP_V8 does not show a clear advantage during any month. In November, the results across all stations were nearly identical.

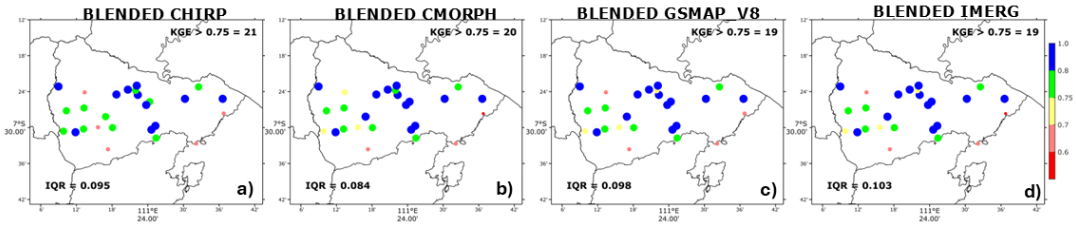

Figure 7 KGE for all monthly data series of RR-Blended (a) bCHIRP, (b) bCMORPH, (c) b GSMAP_V8, and (d) bIMERG

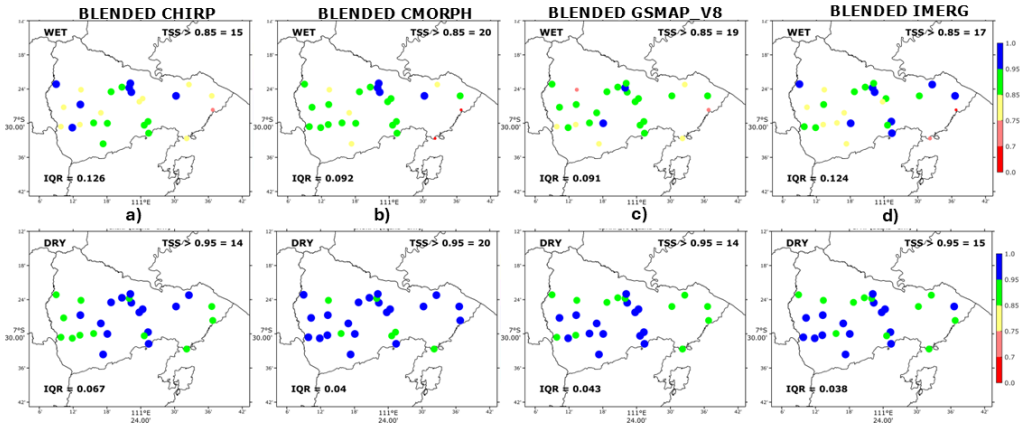

Figure 8 TSS of the RR-Blended data series in the WET (top panel row) and DRY (bottom panel row) periods.

3.5 Spatial Assessment

Spatially, the results from the four RR-Blended datasets indicate that KGE values exceed 0.75 at the majority of rain gauges. As shown in Figure 7, bCHIRP and bCMORPH exhibit superior accuracy at 21 and 20 rain gauges, respectively. The interquartile range (IQR) for the KGE values of these two satellites are as follows: IQR for bCHIRP = 0.095 and IQR for bCMORPH = 0.084, which suggests a higher level of performance compared to the other two satellites. A smaller IQR indicates reduced variability, implying that the KGE values are more consistent across the rainfall gauges.

Figure 8 illustrates that all four satellites generally produce TSS values greater than 0.85. Notably, TSS values during the DRY period tend to be higher than those observed during the WET period. This difference can be attributed to the relatively low rainfall variability during the DRY period, which facilitates more accurate predictions. As a result, the TSS thresholds for the DRY (threshold = 0.95) and WET (threshold = 0.85) periods differ slightly to account for the varying influence of the satellites. During the WET period, bCMORPH consistently yields the highest TSS values, exceeding 0.85 at 20 rain gauges, alongside the lowest IQR of 0.092, indicating a narrow range of TSS values across the gauges. In the DRY period, bCMORPH demonstrates superior performance compared to the other satellites, with 20 rain gauges registering TSS values exceeding 0.95 and an IQR of 0.04.

4. DISCUSSION

4.1 RR-Blended-Weighted

The results suggest that no single satellite can be considered superior for estimating monthly rainfall in the Ngawi Region. While bCMORPH exhibits strong performance in the spatial assessment (Figure 8), this advantage does not carry over to the monthly assessment, as shown in Table 3. Therefore, we utilized the normalized TSS value presented in Table 3 as the weighting factor for each month. The use of TSS as a weight is considered more appropriate than KGE, as TSS accounts for both the coefficient of variation and the correlation between models (Yang et al., 2020). By multiplying the weighted values of each RR-Blended dataset by the corresponding monthly RR-Blended rainfall, a new dataset, termed RR-Blended-Weighted, was generated. This dataset was then re-evaluated alongside the original RR-Blended datasets from each satellite. The findings reveal that the RR-Blended-Weighted dataset outperforms the original RR-Blended dataset across all four-evaluation metrics (Figure 9).

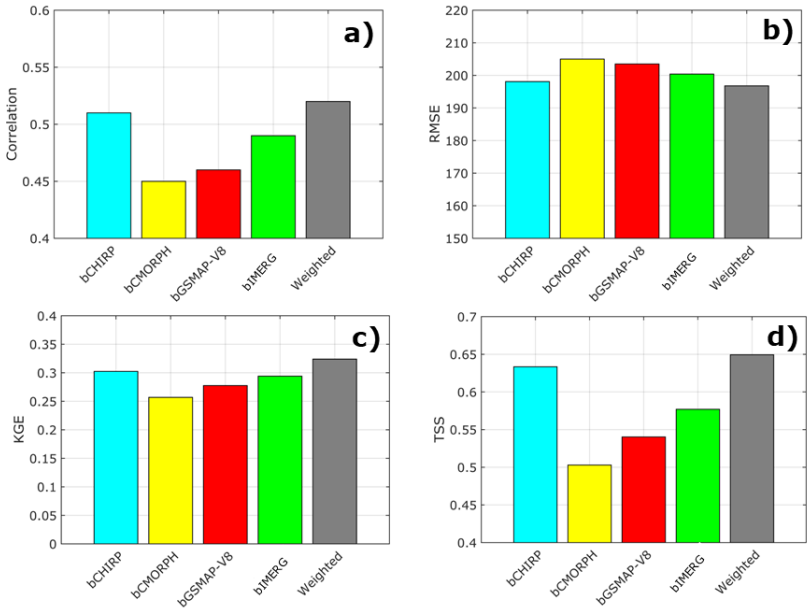

Figure 9 Comparison of the RR-Blended and RR-Blended-Weighted Skill Scores

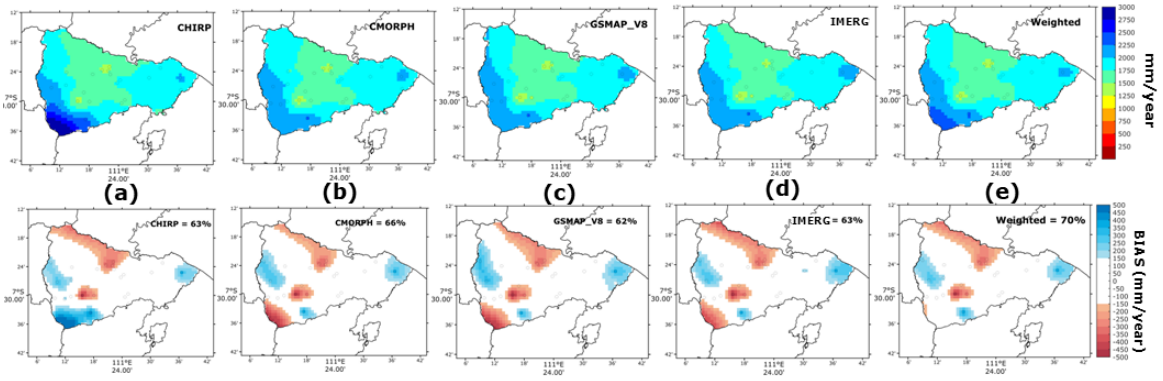

Figure 10 Annual rainfall of RR-Blended for each satellite (a-d) and RR-Blended-Weighted (e) of Ngawi Region. The top panel is the annual accumulation and the bottom panel is the difference with the SAOBS data.

4.2 RR-Blended-Weighted as a Gridded Dataset for the Ngawi Region

Finally, a gridded dataset for Ngawi was obtained, which was regarded as the most accurate estimate. Rather than employing a single satellite as a reference for generating a gridded dataset, we integrate scores from four satellites, applying the weights specified in Table 3 to produce RR-Blended-Weighted. The gridded dataset has a resolution of 0.01° x 0.01°, enabling a more precise representation

of the rainfall details in Ngawi. The gridded RR-Blended for the annual rainfall climatology shows no significant spatial differences among the various dataset. Figure 10 illustrates the significant precipitation levels in southwest Ngawi. bCHIRP indicates an annual RR accumulation ranging from 2500 to 3000 mm/year, the highest recorded among another RR-Blended dataset. RR-Blended-Weighted results in a slight reduction of the total annual rainfall in this region to 2000 - 2500 mm/year.

To confirm that the accuracy of this RR-Blended-Weighted exceeds that of the single RR-Blended, we utilized the Southeast Asia Observation (SAOBS) data as a validation tool. SAOBS is a gridded dataset derived from terrestrial rainfall observations, including data from rain gauges and BMKG stations, which are interpolated through an objective analysis methodology (van den Besselaar et al., 2017). SAOBS exhibits a spatial resolution of 0.25° x 0.25°, which is comparatively lower than that of satellite observation dataset like CHIRP, CMORPH, and GSMAP_V8. The SA-OBS data can be accessed via the BMKG SACAD website[1]. The validation results indicate that RR-Blended-Weighted exhibits a lower bias when assessed with the SAOBS data, which was initially adjusted to match the grid size of RR-Blended. The bias value falls within the low category, defined as an absolute bias of less than 150 mm/year or an assumed value of 25 mm/month. The Ngawi area exhibited a low bias in the RR-Blended dataset, specifically bCHIRP, bCMORPH, b GSMAP_V8, and bIMERG, with values of 63%, 66%, 62%, and 63%, respectively. In the case of the RR-Blended-Weighted variant, the area percentage attained was 70%, the highest among the four other RR-Blended variants.

The results indicate that the RR-Blended grid dataset merging approach yields more optimal outcomes than using the dataset independently for constructing a grid blending dataset for Ngawi. Although our study is limited to the Ngawi Region, we assert that the processes and findings can be replicated in broader contexts. The insights gained from this research may serve as recommendations for BMKG operational institutions to adopt the RR-Blended weighting technique, potentially enhancing the quality of monthly rainfall grid dataset compared to existing methods.

5. CONCLUSION

This study has demonstrated that the application of the *KED* interpolation method, utilizing blended satellite and ground-based rainfall data, significantly enhances the accuracy of monthly rainfall estimation in the Ngawi region. By integrating four satellite-based rainfall products, namely CHIRP, CMORPH, GSMAP_V8, and IMERG with observational data from 26 rain gauge stations, the resulting gridded rainfall dataset exhibited superior performance in representing both spatial and temporal rainfall variability, compared to estimates derived solely from satellite observations. The *KED*-based blending approach effectively reduced systematic bias and root mean square error (RMSE), particularly during the rainy season, where satellite-only data often displayed substantial deviations from ground observations.

Among the four blended dataset, the CHIRP-based product (bCHIRP) yielded the most accurate estimation of total annual rainfall, as evidenced by a comprehensive evaluation of error metrics. Temporally, bCHIRP, bCMORPH, and bIMERG demonstrated consistent performance across all months, while b GSMAP_V8, although not dominant in any particular month, produced results that were relatively comparable. In terms of seasonal detection, especially the identification of the onset and intensity of the rainy season, bCMORPH provided the highest alignment with observed rainfall patterns. Spatially, bCMORPH also performed best across numerous rain gauge locations during both wet and dry periods.

In conclusion, the *KED*-based blending approach has proven effective in generating more accurate and operationally useful monthly rainfall data for the Ngawi region. The findings of this study are expected to support BMKG in the selection and application of satellite data for operational rainfall estimation, particularly in regions with sparse observational coverage. For future research, it is recommended to investigate the integration of additional auxiliary variables such as topographic data, land surface characteristics, or radar-based rainfall estimates. Moreover, extending the methodology to

[1] https://sacad.bmkg.go.id/

higher temporal resolutions (e.g., daily or sub-daily) and applying it across broader geographic regions could further validate the robustness and applicability of the *KED* approach for diverse hydrometeorological conditions in Indonesia.

ACKNOWLEDGMENT

Author thanks to Pusat Pengembangan Sumber Daya Manusia Badan Meteorologi, Klimatologi, dan Geofisika (PPSDM BMKG) for funding this research with Contract Number e.B/HM.02.03/001/KDL/I/2024. We also thank the National Aeronautics and Space Administration (NASA), Climate Hazards Center University of California, National Oceanic and Atmospheric Administration (NOAA), and the Japan Aerospace Exploration Agency (JAXA) for providing satellite data used in this study.

REFERENCE

Aldrian, E., & Dwi Susanto, R. (2003). Identification of three dominant rainfall regions within Indonesia and their relationship to sea surface temperature. *International Journal of Climatology*, *23*(12), 1435–1452. https://doi.org/10.1002/joc.950

Bai, L., Shi, C., Li, L., Yang, Y., & Wu, J. (2018). Accuracy of CHIRPS satellite-rainfall products over mainland China. *Remote Sensing*, *10*(3). https://doi.org/10.3390/rs10030362

Beck, H. E., Vergopolan, N., Pan, M., Levizzani, V., Van Dijk, A. I. J. M., Weedon, G. P., Brocca, L., Pappenberger, F., Huffman, G. J., & Wood, E. F. (2017). Global-scale evaluation of 22 precipitation datasets using gauge observations and hydrological modeling. *Hydrology and Earth System Sciences*, *21*(12), 6201–6217. https://doi.org/10.5194/hess-21-6201-2017

BMKG. (2021). *Buku Peta Rata-rata Curah Hujan dan Hari Hujan Periode 1991-2020 Indonesia*. BMKG. https://iklim.bmkg.go.id/bmkgadmin/storage/buletin/20220511_BukuNormal_Lengkap_FormatBuku.pdf

Cantet, P. (2017). Mapping the mean monthly precipitation of a small island using kriging with external drifts. *Theoretical and Applied Climatology*, *127*(1–2), 31–44. https://doi.org/10.1007/s00704-015-1610-z

Chappell, A., Renzullo, L. H., Raupach, T. J., & Haylock, M. (2013). Evaluating geostatistical methods of blending satellite and gauge data to estimate near real-time daily rainfall for Australia. *Journal of Hydrology*, *493*, 105–114. https://doi.org/10.1016/j.jhydrol.2013.04.024

Chua, Z. W., Kuleshov, Y., Watkins, A. B., Choy, S., & Sun, C. (2022). A Two-Step Approach to Blending GSMaP Satellite Rainfall Estimates with Gauge Observations over Australia. *Remote Sensing*, *14*(8). https://doi.org/10.3390/rs14081903

Fatkhuroyan, & TrinahWati. (2018). Accuracy Assessment of Global Satellite Mapping of Precipitation (GSMaP) Product over Indonesian Maritime Continent. *IOP Conference Series: Earth and Environmental Science*, *187*(1). https://doi.org/10.1088/1755-1315/187/1/012060

Funk, C., Peterson, P., Landsfeld, M., Pedreros, D., Verdin, J., Shukla, S., Husak, G., Rowland, J., Harrison, L., Hoell, A., & Michaelsen, J. (2015). The climate hazards infrared precipitation with stations - A new environmental record for monitoring extremes. *Scientific Data*, *2*. https://doi.org/10.1038/sdata.2015.66

Goshime, D. W., Absi, R., & Ledésert, B. (2019). Evaluation and bias correction of CHIRP rainfall estimate for rainfall-runoff simulation over Lake Ziway Watershed, Ethiopia. *Hydrology*, *6*(3). https://doi.org/10.3390/hydrology6030068

Groisman, P. ya, & Legates, D. R. (1994). The Accuracy SS of United States Precipitation Data. *Bulletin of the American Meteorological Society*, *75*(3), 215–228. https://doi.org/10.1175/1520-0477(1994)075<0215:TAOUSP>2.0.CO;2

Hengl, T., Heuvelink, G. B. M., & Stein, A. (2003). Comparison of kriging with external drift and regression-kriging *. In *ITC, Technical Note*. ITC, Technical Note. http://www.itc.nl/library/Academic

Hou, A. Y., Kakar, R. K., Neeck, S., Azarbarzin, A. A., Kummerow, C. D., Kojima, M., Oki, R., Nakamura, K., & Iguchi, T. (2014). The global precipitation measurement mission. *Bulletin of the American Meteorological Society*, *95*(5), 701–722. https://doi.org/10.1175/BAMS-D-13-00164.1

Huffman, G. J., Bolvin, D. T., Nelkin, E. J., & Tan, J. (2019). Integrated Multi-satellitE Retrievals for GPM (IMERG) Technical Documentation. In *IMERG Tech Document*.

Jewell, S. A., & Gaussiat, N. (2015). An assessment of kriging-based rain-gauge-radar merging techniques. *Quarterly Journal of the Royal Meteorological Society*, *141*(691), 2300–2313. https://doi.org/10.1002/qj.2522

Jiang, Q., Li, W., Wen, J., Fan, Z., Chen, Y., Scaioni, M., & Wang, J. (2019). Evaluation of satellite-based products for extreme rainfall estimations in the eastern coastal areas of China. *Journal of Integrative Environmental Sciences*, *16*(1), 191–207. https://doi.org/10.1080/1943815X.2019.1707233

Joyce, R. J., Janowiak, J. E., Arkin, P. A., & Xie, P. (2004). CMORPH: A Method that Produces Global Precipitation Estimates from Passive Microwave and Infrared Data at High Spatial and Temporal Resolution. *Journal of Hydrology*, *5*(3), 487–503. https://doi.org/https://doi.org/10.1175/1525-7541(2004)005<0487:CAMTPG>2.0.CO;2

Knoben, W. J. M., Freer, J. E., & Woods, R. A. (2019). Technical note: Inherent benchmark or not? Comparing Nash-Sutcliffe and Kling-Gupta efficiency scores. *Hydrology and Earth System Sciences*. https://doi.org/10.5194/hess-2019-327

Kubota, T., Shige, S., Hashizume, H., Aonashi, K., Takahashi, N., Seto, S., Hirose, M., Takayabu, Y. N., Ushio, T., Nakagawa, K., Iwanami, K., Kachi, M., & Okamoto, K. (2007). Global precipitation map using satellite-borne microwave radiometers by the GSMaP project: Production and validation. *IEEE Transactions on Geoscience and Remote Sensing*, *45*(7), 2259–2275. https://doi.org/10.1109/TGRS.2007.895337

Lin, A., & Wang, X. L. (2011). An algorithm for blending multiple satellite precipitation estimates with in situ precipitation measurements in Canada. *Journal of Geophysical Research Atmospheres*, *116*(21). https://doi.org/10.1029/2011JD016359

Ly, S., Charles, C., & Degré, A. (2011). Geostatistical interpolation of daily rainfall at catchment scale: The use of several variogram models in the Ourthe and Ambleve catchments, Belgium. *Hydrology and Earth System Sciences*, *15*(7), 2259–2274. https://doi.org/10.5194/hess-15-2259-2011

Mathevet, T., Le Moine, N., Andréassian, V., Gupta, H., & Oudin, L. (2023). Multi-objective assessment of hydrological model performances using Nash–Sutcliffe and Kling–Gupta efficiencies on a worldwide large sample of watersheds. *Comptes Rendus - Geoscience*, *355*. https://doi.org/10.5802/crgeos.189

Michaelides, S., Levizzani, V., Anagnostou, E., Bauer, P., Kasparis, T., & Lane, J. E. (2009). Precipitation: Measurement, remote sensing, climatology and modeling. *Atmospheric Research*, *94*(4), 512–533. https://doi.org/10.1016/j.atmosres.2009.08.017

Michelson, D. B. (2004). Systematic correction of precipitation gauge observations using analyzed meteorological variables. *Journal of Hydrology*, *290*(3–4), 161–177. https://doi.org/10.1016/j.jhydrol.2003.10.005

Muharsyah, R., Fitria Kussatiti, D., Ripaldi, A., Maharani, T., Nur Ratri, D., Hanif Damayanti, R., Denata, M., Yuswantoro, A., & Wahyuni, N. (2021). Mengukur Penambahan Curah Hujan pada 34 Provinsi di Indonesia saat Periode La Nina Menggunakan Blending Curah Hujan Pengamatan In-Situ Dan Satelite (Measuring Rainfall Increament Over 34 Provinces in Indonesia During La Nina Period using Blending Rainfall In-Situ and Satellite Observation). *Seminar Nasional Geomatika BIG*.

Mulsandi, A., Koesmaryono, Y., Hidayat, R., Faqih, A., & Sopaheluwakan, A. (2024). Detecting Indonesian Monsoon Signals and Related Features Using Space–Time Singular Value Decomposition (SVD). *Atmosphere*, *15*(2), 1–15. https://doi.org/10.3390/atmos15020187

Murphy, B., Yurchak, R., & Müller, S. (2024). *GeoStat-Framework/PyKrige: v1.7.2*. https://doi.org/https://doi.org/10.5281/zenodo.11360184

Nanding, N., Rico-Ramirez, M. A., & Han, D. (2015). Comparison of different radar-raingauge rainfall merging techniques. *Journal of Hydroinformatics*, *17*(3), 422–445. https://doi.org/10.2166/hydro.2015.001

Novia Nur Rohma. (2022). Estimation of Ordinary Kriging Method with Jackknife Technique on Rainfall Data in Malang Raya. *International Journal on Information and Communication Technology (IJoICT)*, *8*(2), 22–39. https://doi.org/10.21108/ijoict.v8i2.678

Oliver, M. A., & Webster, R. (2015). *Springer Briefs in Agriculture Basic Steps in Geostatistics: The Variogram and Kriging*. Springer. https://doi.org/DOI10.1007/978-3-319-15865-5

Pang, Y., Wang, Y., Lai, X., Zhang, S., Liang, P., & Song, X. (2023). Enhanced Kriging leave-one-out cross-validation in improving model estimation and optimization. *Computer Methods in Applied Mechanics and Engineering*, *414*. https://doi.org/10.1016/j.cma.2023.116194

Peterson, T. C., Easterling, D. R., Karl, T. R., Groisman, P., Nicholls, N., Plummer, N., Torok, S., Auer, I., Boehm, R., Gullett, D., Vincent, L., Heino, R., Tuomenvirta, H., Mestre, O., Tama´, T., Szentimrey, T., Salinger, J., Førland, E. J., Hanssen-Bauer, I., … Parker, D. (1998). A review. International Journal of Climatology: *A Journal of the Royal Meteorological Society*, 18(13), 1493-1517.

Pratama, A., Agiel, H. M., & Oktaviana, A. A. (2022). Evaluasi Satellite Precipitation Product (GSMaP, CHIRPS, dan IMERG) di Kabupaten Lampung Selatan. *Journal of Science and Applicative Technology*, *6*(1), 32. https://doi.org/10.35472/jsat.v6i1.702

Pririzki, S. J., Sari, N., Agustin, B., Razaf, Y., & Simbolon, E. (2022). Penerapan Model Semivariogram Eksperimental Pada Curah Hujan Bulanan Di Indonesia (Application of Experimental Semivariogram Model on Monthly Rainfall In Indonesia). *Jurnal Fraction*, *2*(1), 1–7.

Ramadhan, R., Marzuki, M., Yusnaini, H., Muharsyah, R., Tangang, F., Vonnisa, M., & Harmadi, H. (2023). A Preliminary Assessment of the GSMaP Version 08 Products over Indonesian Maritime Continent against Gauge Data. *Remote Sensing*, *15*(4). https://doi.org/10.3390/rs15041115

Ramadhan, R., Marzuki, M., Yusnaini, H., Muharsyah, R., Suryanto, W., Sholihun, S., Vonnisa, M., Battaglia, A., & Hashiguchi, H. (2022). Capability of GPM IMERG Products for Extreme Precipitation Analysis over the Indonesian Maritime Continent. *Remote Sensing*, *14*(2). https://doi.org/10.3390/rs14020412

Shen, G., Chen, N., Wang, W., & Chen, Z. (2019). WHU-SGCC: A novel approach for blending daily satellite (CHIRP) and precipitation observations over the Jinsha River basin. *Earth System Science Data*, *11*(4), 1711–1744. https://doi.org/10.5194/essd-11-1711-2019

Sideris, I. V., Gabella, M., Erdin, R., & Germann, U. (2014). Real-time radar-rain-gauge merging using spatio-temporal co-kriging with external drift in the alpine terrain of Switzerland. *Quarterly Journal of the Royal Meteorological Society*, *140*(680), 1097–1111. https://doi.org/10.1002/qj.2188

Taylor, K. E. (2001). Summarizing multiple aspects of model performance in a single diagram. *Journal of Geophysical Research Atmospheres*, *106*(D7), 7183–7192. https://doi.org/10.1029/2000JD900719

van den Besselaar, E. J. M., van der Schrier, G., Cornes, R. C., Suwondo, A., Iqbal, & Tank, A. M. G. K. (2017). SA-OBS: A daily gridded surface temperature and precipitation dataset for Southeast Asia. *Journal of Climate*, *30*(14), 5151–5165. https://doi.org/10.1175/JCLI-D-16-0575.1

Verdin, A., Rajagopalan, B., Kleiber, W., & Funk, C. (2015). A Bayesian kriging approach for blending satellite and ground precipitation observations. *Water Resources Research*, *51*(2), 908–921. https://doi.org/10.1002/2014WR015963

Vernimmen, R. R. E., Hooijer, A., Mamenun, Aldrian, E., & Van Dijk, A. I. J. M. (2012). Evaluation and bias correction of satellite rainfall data for drought monitoring in Indonesia. *Hydrology and Earth System Sciences*, *16*(1), 133–146. https://doi.org/10.5194/hess-16-133-2012

Wati, T., Hadi, T. W., Sopaheluwakan, A., & Hutasoit, L. M. (2021). Evaluation gridded precipitation datasets in Indonesia. *IOP Conference Series: Earth and Environmental Science*, *893*(1). https://doi.org/10.1088/1755-1315/893/1/012056

Yang, X., Yu, X., Wang, Y., He, X., Pan, M., Zhang, M., Liu, Y. I., Ren, L., & Sheffield, J. (2020). The Optimal Multimodel Ensemble of Bias-Corrected CMIP5 Climate Models over China. *Journal of Hydrometeorology*, *21*, 845–863. https://doi.org/10.1175/JHM-D-19